Electronic Supplementary Information (ESI) for

Evidence of a reversible redox reaction in a liquid-electrolyte-type fluoride-ion battery

Ritsuko Yaokawa, Tohru Shiga, Shinya Moribe and Kazuhiko Mukai

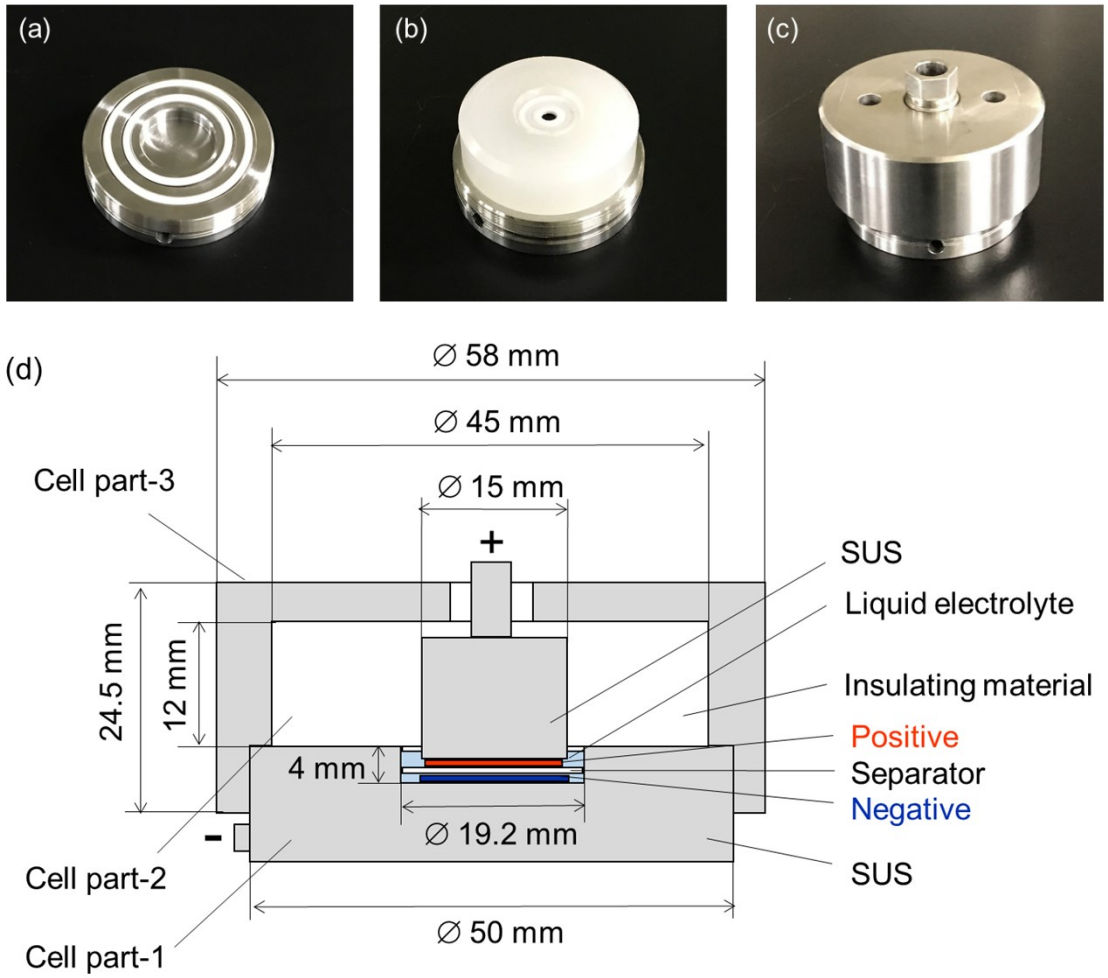

Fig. S1: (a)–(c) Photographs and (d) schematic structure of the hermetically sealed cell in this study. The cell consisted of stainless steel (SUS) as the outer material (parts 1 and 3), PTFE as the insulating material (part 2), and the contents of the electrodes. The diameters of the positive and negative electrodes were 14 and 16 mm, respectively. This cell was designed and fabricated in our laboratory.

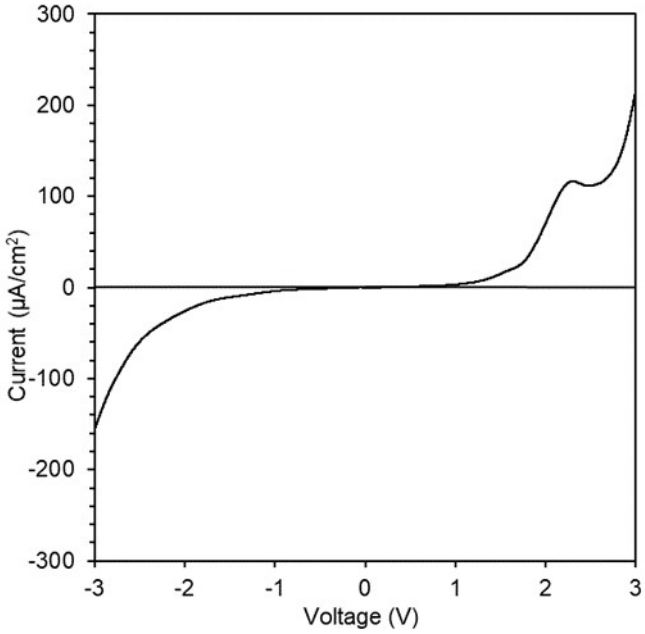

Fig. S2: LSV curve of the Pt|TEAF/PC|Pt cell operated at a scan rate of 1 mV s^{-1}.

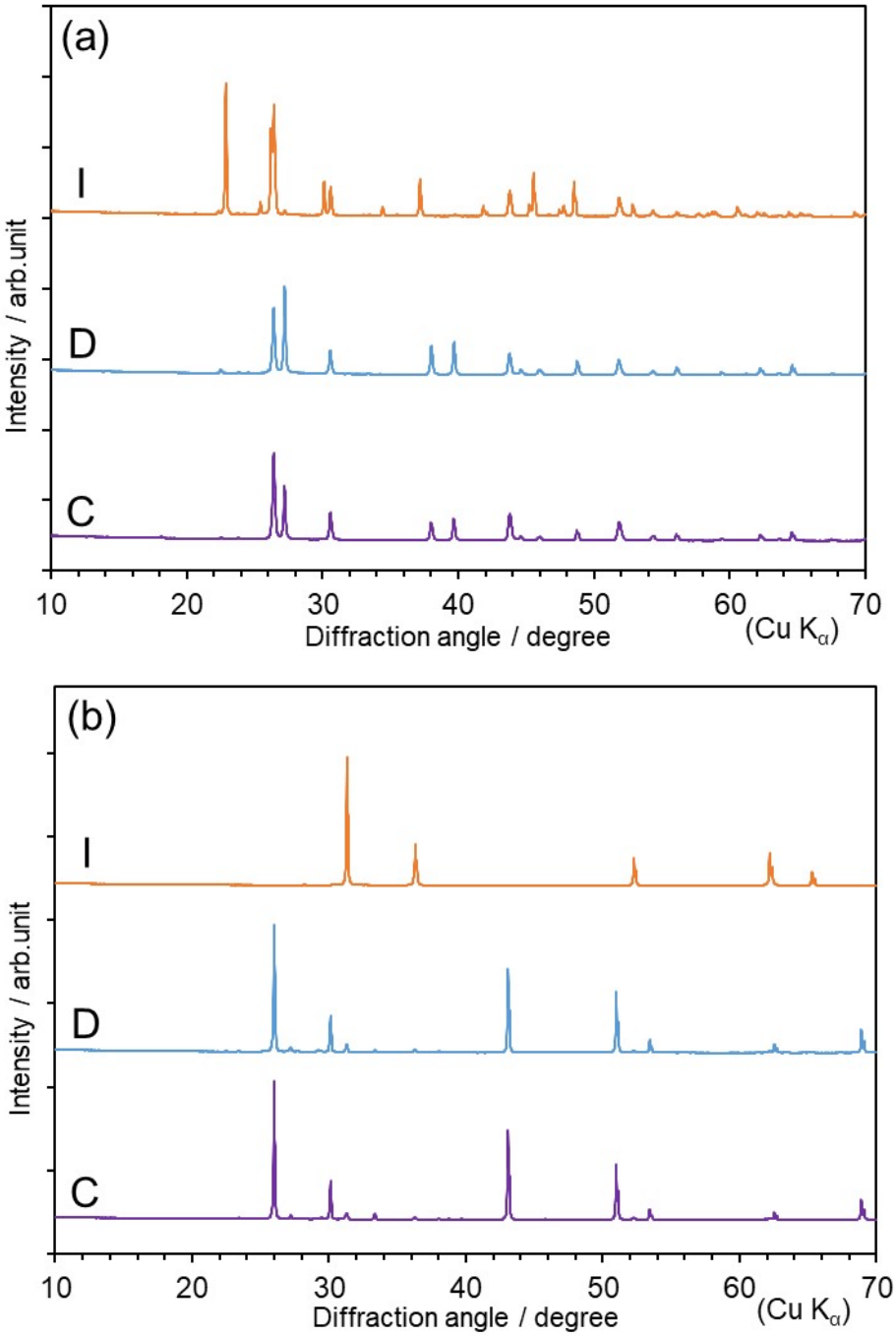

Fig. S3: Full-2θ range *ex situ* XRD patterns of the

BiF_3|TEAF/PC|Pb-plate cell at **I**, **D**, and **C:** (a) BiF_3 and (b) Pb-plate electrodes. The XRD patterns in (a) and (b) are essentially same with those in Figs. 1(b) and 1(c), respectively.

Table S1: Lattice parameters of the BiF_3, Bi, Pb, and PbF_2 phases calculated from the patterns for **I**, **D**, and **C** in Fig. S3, including their reported values in the ICDD database accessed using PDF-4+ 2018 software

State	Electrode or PDF-4+ No.	Phase	Crystal system	Lattice parameters/Å
I	positive	BiF_3	cubic	$a_c = 5.827$
		BiF_3	orthorhombic	$a_o = 6.559$
				$b_o = 6.951$
				$c_o = 4.844$
	negative	Pb	cubic	$a_c = 4.945$
D	positive	BiF_3	cubic	$a_c = 5.824$
		Bi	rhombohedral	$a_h = 4.541$
				$c_h = 11.84$
	negative	PbF_2	cubic	$a_c = 5.934$
C	positive	BiF_3	cubic	$a_c = 5.847$
		Bi	rhombohedral	$a_h = 4.541$
				$c_h = 11.86$
	negative	PbF_2	cubic	$a_c = 5.934$
Reported values	04-007-1470	BiF_3	cubic	$a_c = 5.853$
	04-005-4815	BiF_3	orthorhombic	$a_o = 6.561$
				$b_o = 7.015$
				$c_o = 4.841$
	98-000-0118	Bi	rhombohedral	$a_h = 4.546$
				$c_h = 11.86$
	98-000-0279	Pb	cubic	$a_c = 4.951$
	00-006-0251	PbF_2	cubic	$a_c = 5.940$

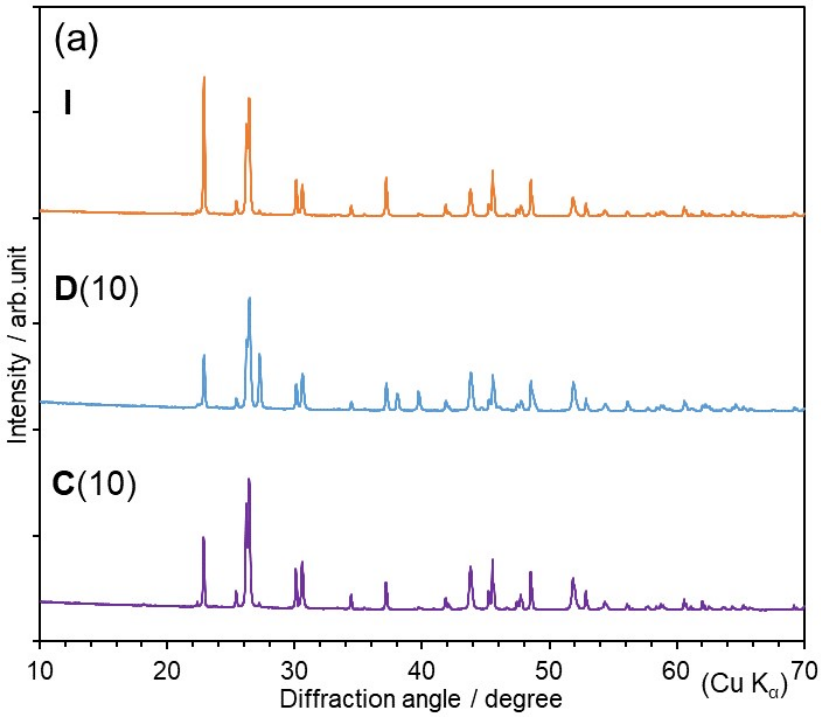
(a)
I
D(10)
C(10)
Intensity / arb.unit
10
20
30
40
50
60
70
(Cu Kα)
Diffraction angle / degree

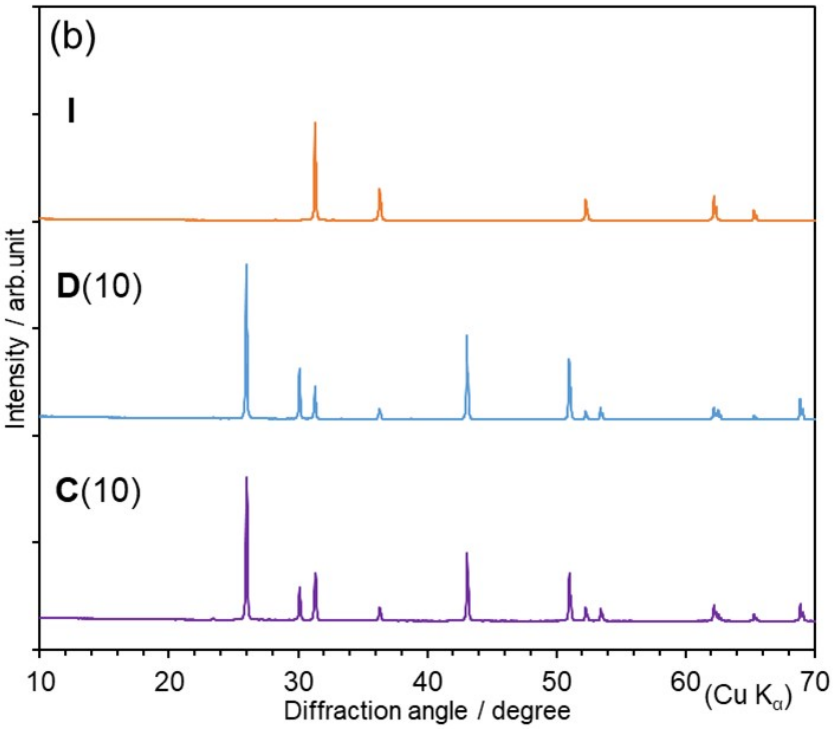
(b)
I
D(10)
C(10)
Intensity / arb.unit
10
20
30
40
50
60
70
(Cu Kα)
Diffraction angle / degree

Fig. S4: Full-2θ range *ex situ* XRD patterns of the BiF_3|TEAF/PC|Pb-plate cell at **I**, **D**(10), and **C**(10): (a) BiF_3 and (b) Pb-plate electrodes. The XRD patterns in (a) and (b) are essentially same with those in Figs. 2(b) and 2(c), respectively.

Table S2: Lattice parameters of the BiF_3, Bi, Pb, and PbF_2 phases calculated from the patterns for **D**(10) and **C**(10) in Fig. S5

State	Electrode	Phase	Crystal system	Lattice parameters/Å
D(10)	positive	BiF_3	cubic	a_c = 5.843
		BiF_3	orthorhombic	a_o = 6.555
				b_o = 6.951
				c_o = 4.845
		Bi	rhombohedral	a_h = 4.551
				c_h = 11.83
	negative	Pb	cubic	a_c = 4.945
		PbF_2	cubic	a_c = 5.935
C(10)	positive	BiF_3	cubic	a_c = 5.824
		BiF_3	orthorhombic	a_o = 6.558
				b_o = 6.951
				c_o = 4.851
	negative	Pb	cubic	a_c = 4.940
		PbF_2	cubic	a_c = 5.934

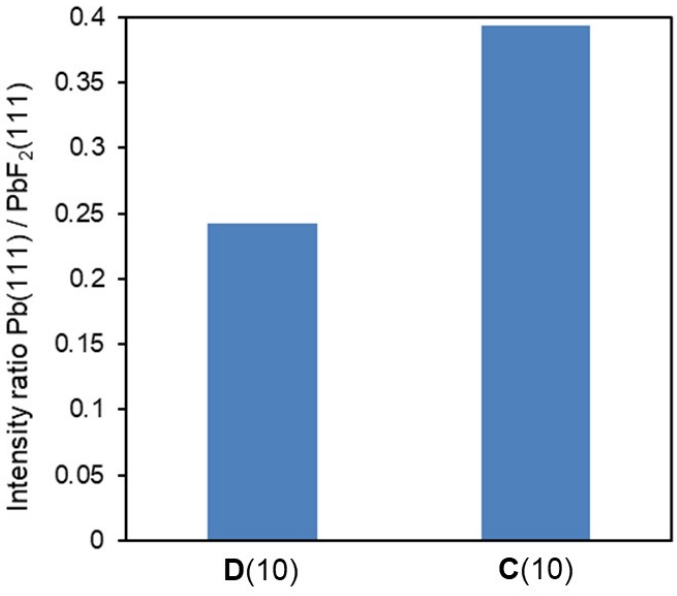

Fig. S5: Intensity ratios of the Pb(111) and PbF_2(111) diffraction lines in Fig. 2(c).

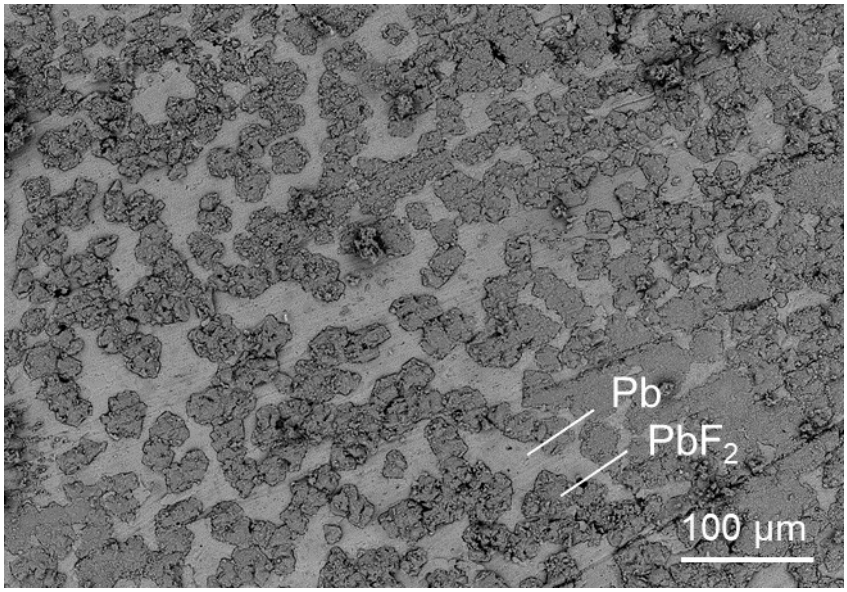

Fig. S6: BSE image of the Pb plate at **D**(10).

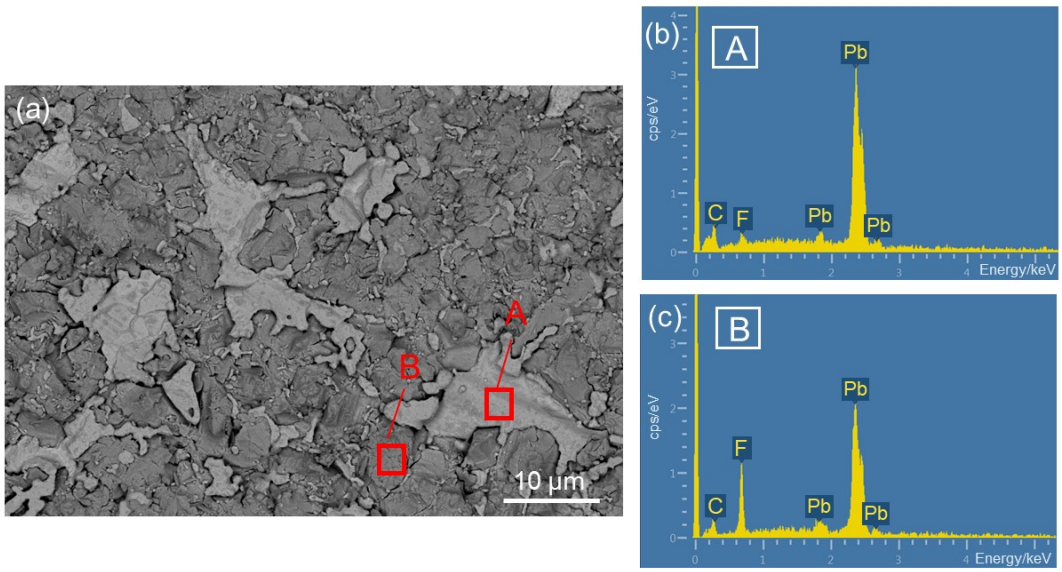

Fig. S7: (a) BSE image of the surface of the Pb-plate electrode at **C**(10). EDX spectra from the areas (b) A and (c) B in (a).

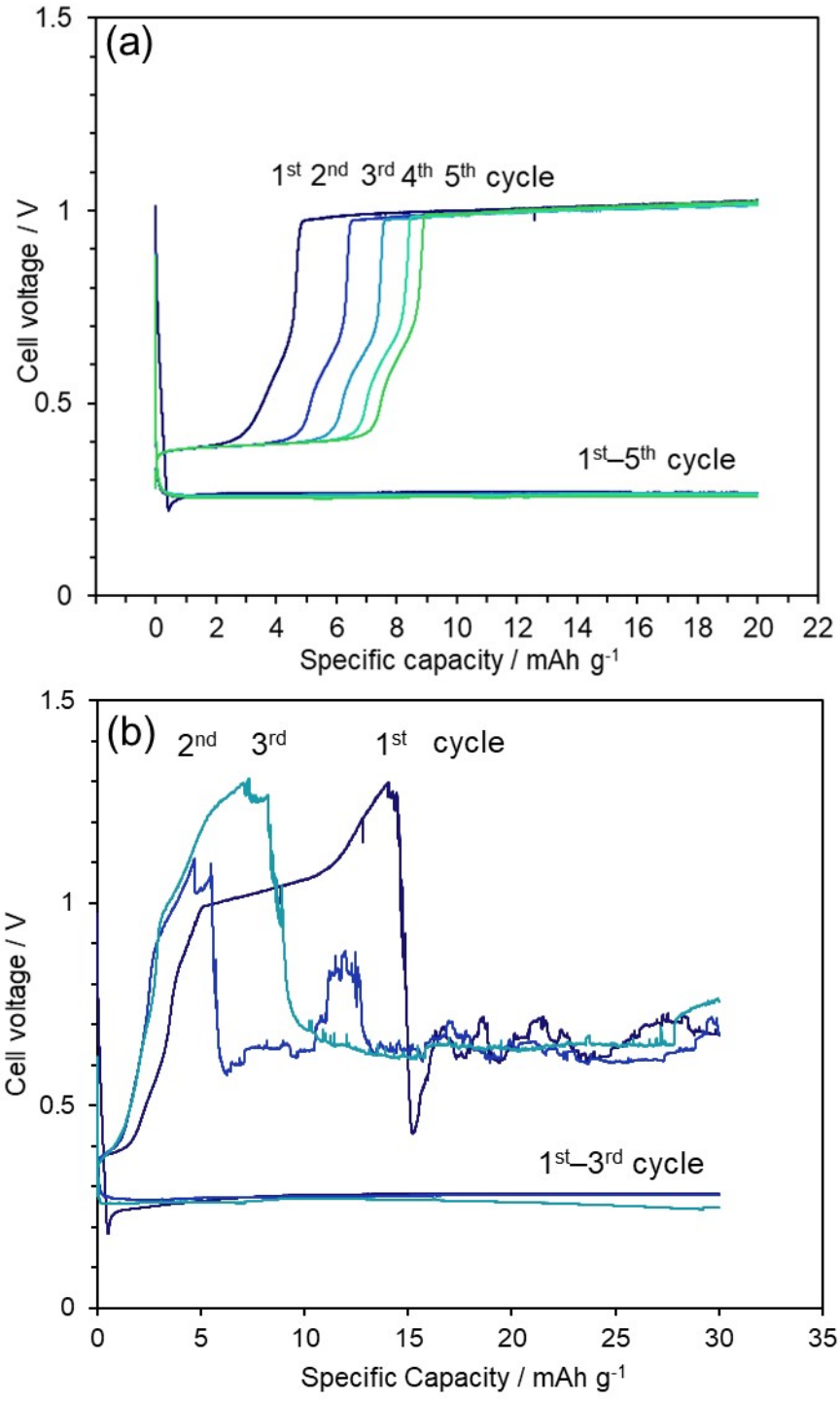

Fig. S8: *Q*-limited discharge and charge curves of the BiF_3|TEAF/PC|Pb-plate cells: (a) Q = 20 mAh g^{-1} and (b) Q = 30 mAh g^{-1}.

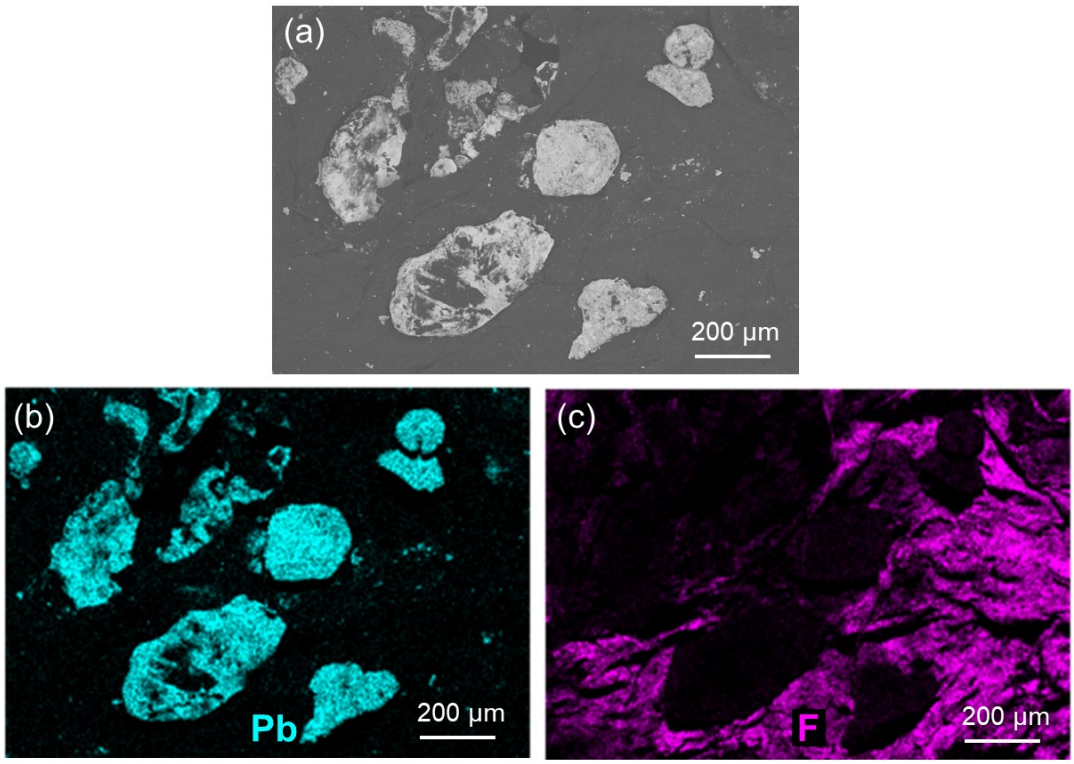

Fig. S9: (a) BSE image of the Pb powder at **C**(*rcv*) and EDX mappings of (b) Pb and (c) F.

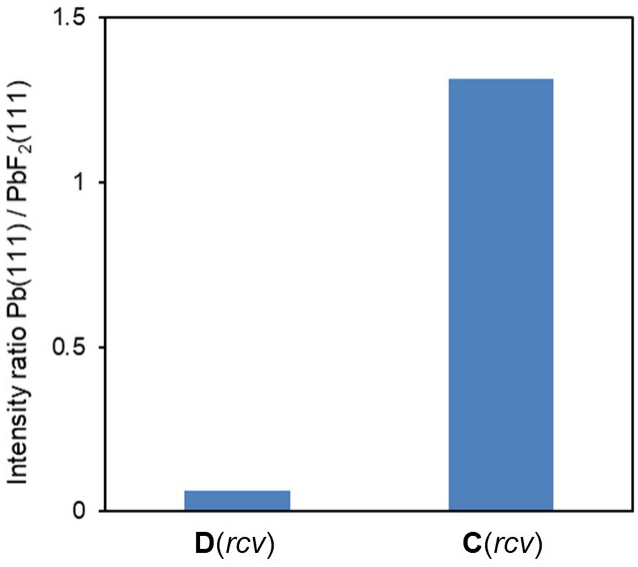

Fig. S10: Intensity ratios of the Pb(111) and PbF_2(111) diffraction lines in Fig. 3(c).

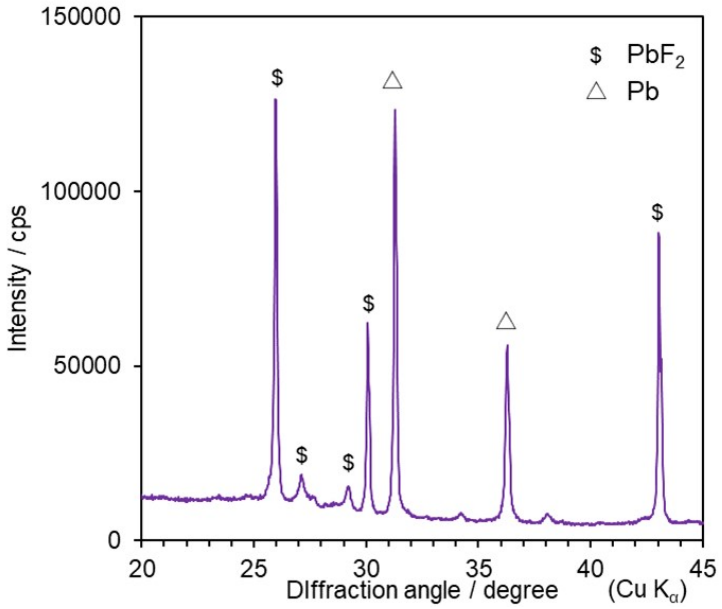

Fig. S11: *Ex situ* XRD pattern of the *α*-Pb electrode from the BiF_3|TEAF/PC|*α*-Pb cell after the discharge and charge reactions. $ and △ represent the diffraction lines from the PbF_2 and Pb Phases, respectively.